

Antifungal Properties of High Efficient W/WO₃ Electrodes Acting under UV-Vis and Visible Light and Chloride Medium

Barbara C. A. Souza,^a Thais T. Guaraldo,^a Michelle F. Brugnera,^b Regina H. Pires,^c
Maria J. S. M. Giannini^c and Maria V. B. Zanoni^{*,a}

^aDepartamento de Química Analítica, Instituto de Química, UNESP,
Rua Francisco Degni, 55 Bairro Quitandinha, 14800-900 Araraquara-SP, Brazil

^bDepartamento de Química, Universidade Federal de Mato Grosso (UFMT),
78060-900 Cuiabá-MT, Brazil

^cDepartamento de Análises Clínicas, Faculdade de Ciências Farmacêuticas, UNESP,
Rodovia Araraquara-Jaú, km 01, 14801-902 Araraquara-SP, Brazil

The present work investigates the use of W/WO₃ electrodes prepared by electrochemical anodization applied in the photoelectrocatalytic disinfection of *Candida parapsilosis* using ultraviolet-visible (UV-Vis) and visible irradiation. The core objective of this work lies in describing a novel approach involving the use of chloride as supporting electrolyte, aiming at achieving a faster inactivation and towards understanding its behavior in water containing high chloride content. The best experimental conditions were found to be at pH 7.0 and 0.1 mol L⁻¹ NaCl when the photoelectrode was biased at 1.5 V (vs. Ag/AgCl) illuminated by both UV-Vis and visible light. It is suggested that charges photogenerated on the electrode surface give rise preferably to HO•, known to be powerful oxidant that causes the total inactivation of the microorganism (1 min of treatment) while engendering around 84% of mineralization of organic matter released from the cell damage following 120 min of treatment.

Keywords: photoelectrocatalysis, W/WO₃ semiconductor, *C. Parapsilosis* disinfection, photoelectrocatalysis in chloride medium

Introduction

The supply of quality drinking water has been a growing concern for centuries given the scarcity of this natural resource and the appalling rapid deterioration of water sources owing largely to human activities.¹ According to the World Health Organization, contaminated water is mainly responsible for the deaths of 5,000 people *per* day worldwide, mostly in poor countries where most of the cases are associated with microbiological problems.² Among these related cases, microorganisms belonging to the *Fungi* kingdom have drawn a heightened degree of attention in recent times.

Fungi can be defined as eukaryotic organisms with a nuclear membrane delimiting the cell nucleus.^{3,4} They have emerged as the main causes of human diseases, particularly in immunocompromised individuals and hospitalized

patients.⁵ The species belonging to the genus *Candida* have been the most frequently isolated agents in hospital settings and responsible for 80% of fungal infections contracted in hospitals.^{5,6}

In particular, *Candida parapsilosis* is the second etiologic agent most frequently isolated in blood cultures.^{5,7} It is widely known to affect immunocompromised individuals including AIDS patients, surgical patients and those who require prolonged use of intravenous catheter, such as dialysis and cancer patients with an increased risk of infection from *C. parapsilosis* known as candidiasis.^{2,5,7-10} Candidiasis may result in the formation of micro hepatosplenic kidney abscesses, endocarditis, meningitis, arthritis, osteomyelitis, among others^{11,12} and is considered the major cause of mortality in hemodialysis treatment in patients who use huge amounts of drinking water for “artificial kidney” operation.¹³ Recently, the occurrence of *Candida* spp. has been reported accounting for 102 positive blood cultures in a hospital in Malaysia⁵ of which

*e-mail: mvboldrin@gmail.com

51% were identified as *C. parapsilosis*. In Brazil, it was found that out of 50 blood cultures evaluated, 18 contained *C. parapsilosis*.⁸ By virtue of that, water disinfection based on the removal of this emerging pathogen has been attracting significant attention in an attempt to mitigate this deplorable health situation.

Photoelectrocatalysis is a potentially heterogeneous oxidizing system with high performance in the formation of hydroxyl radicals capable of promoting the degradation of most chemical pollutants while ensuring the complete death of a wide range of microorganisms.¹⁴⁻¹⁹ Examples of photoanodes prepared by different methodologies applied in disinfection using photoelectrocatalysis are shown in Table 1. The results indicate that Ti/TiO₂ is the most used electrode, successfully applied in water disinfection. The biocidal properties of hydroxyl radicals are widely known and their action mechanism lies in their abilities to damage the cell walls in the external shell of microorganisms with further oxidation of the phospholipid components of the membrane.^{18,19,28-30} However, the photoelectrocatalytic method has so far been confronted with some limitations when it comes to the medium containing chloride. Some investigations have revealed that photoelectrocatalysis carried out on Ti/TiO₂ electrode biased at positive potential and illuminated by UV light can generate free chlorine when conducted in medium containing chloride.³¹⁻³⁴

Despite Ti/TiO₂ being the most popular semiconductor

applied in photoelectrocatalysis, the WO₃ has become an excellent alternative material, owing largely to the fact that it presents smaller band gap energy (2.4-2.8 eV) and can be photoexcited in the visible region close to the UV region.³⁵ Nonetheless, most of the studies reported in the literature are found to explore WO₃ essentially as photocatalyst only and employed for the promotion of organic pollutants oxidation.³⁶⁻³⁹ It is noteworthy that no study has been published to date concerning its effect on WO₃ visible light catalytic activity as far as water disinfection is concerned. Further studies ought to be carried out *vis-à-vis* the disinfection in chloride medium using photoelectrocatalysis in order to ensure and perhaps validate its reputation as a cost effective and efficacious treatment method for *Candida* sp. in water media. Accordingly, tests need to be conducted on the use of W/WO₃ photoelectrodes since they can be activated under both UV and visible light illumination.

The aim of the present work lies in assessing the fungicide effect of photoelectrocatalytic oxidation process conducted on W/WO₃ electrodes prepared by electrochemical anodization in chloride medium. The method is tested in the process of *Candida parapsilosis* deactivation and the determination of optimal conditions for the disinfection of fungus in water media enriched with chloride. The degradation of the metabolites released during the cell lysis was monitored by total organic carbon (TOC) measurements.

Table 1. Relevant studies in the literature regarding photoelectrocatalysis and disinfection

Electrode	Synthesis method	Target microorganism	Reference
Ti/TiO ₂	sol-gel method	<i>E. coli</i> <i>Clostridium perfringes</i>	20
Ti/TiO ₂	via thermal	<i>E. coli</i>	21
Ti/TiO ₂	sol-gel method and via thermal	<i>E. coli</i>	16
Fe doped with TiO ₂	sol-gel method and via thermal	<i>E. coli</i>	22
Ti/TiO ₂	sol-gel method	<i>E. coli</i>	17
Ti/TiO ₂ (nanotube)	electrochemical anodization	<i>E. coli</i>	23
W/WO ₃	electrochemical anodization	<i>M. aeuruginosa</i>	24
Ti/TiO ₂	TiO ₂ deposition by dip coating	<i>E. coli</i>	25
Ag-TiO ₂ /G and Cu-TiO ₂ /G	chemical deposition and electrodeposition	<i>E. coli</i>	26
Ti/TiO ₂	electrochemical anodization	<i>C. orthopsilosis</i> <i>C. parapsilosis</i>	27
Ag-Ti/TiO ₂ (nanotube)	electrochemical anodization	<i>M. smegmatis</i> <i>M. kansasii</i> <i>M. avium</i>	18
Ti/TiO ₂	titanium botoxide hydrolysis	<i>E. coli</i>	20
Ti/TiO ₂ (nanotube)	electrochemical anodization	<i>M. fortuitum</i> <i>M. chelonae</i> <i>M. abscessus</i>	19

Experimental

Chemicals and materials

The reagents used in this study for the preparation of the solutions were of analytical grade employing distilled water purified through the Milli-Q system (18.2 MΩ cm Millipore). Tungsten foil (Alfa Aesar, 0.25 mm thick, 99.95%) was used as the substrate for oxide film growth.

The ATCC 22019 strains of yeast were initially incubated in Sabouraud dextrose agar, ideal for yeast cultivation. After the growth of the microorganism, a suspension solution of 0.1 mol L⁻¹ of NaCl was prepared. Further, the microorganism concentration was determined by the aid of an optical microscope in a Neubauer chamber while being subsequently transferred to the photoelectrochemical reactor and diluted to the concentrations of interest.

Synthesis of W/WO₃ nanoporous electrode

The W/WO₃ electrode was prepared through the anodization of tungsten foil (Alfa Aesar, 0.25 mm, 99.95%). This foil was laser cut to 4 × 4 cm in size and mechanically polished on SiC sandpaper of successively thinner roughness (800, 1000, 1200, 1500 and 2000). After this treatment, the foil was washed in ultrasonic bath for 5 min in acetone followed by isopropanol and water, and was subsequently dried with N₂ prior to its immediate use. For the experiments, we used an anodizing conventional electrochemical cell of two-electrode, the tungsten foil (4 × 4 cm) as working electrode and a Pt gauze as counter-electrode. A tungsten foil was immersed in NaF solution of 0.15 mol L⁻¹ as supporting electrolyte, applying a ramp potential of 0.2 V s⁻¹ until it reached 60 V, which was maintained for 2 h using a power supply of 60 V/2 A stabilized Tectrol®. After anodizing, the electrode was then carefully washed by immersion in deionized water and dried under N₂ flow. As final treatment, the electrode was annealed at 450 °C for 2 h in line with the procedure described in the literature.^{24,40}

Characterization of W/WO₃ nanoporous electrode

The morphological analysis of W/WO₃ surface was performed by scanning electron microscope FE-SEM high resolution with the source of electrons by field emission, JEOL, model JSM-7500-F and energy dispersive X-ray spectroscopy (EDX). The electrode was electrochemically characterized by linear scan voltammetry using a reactor, sodium sulfate and sodium chloride of 0.10 mol L⁻¹ as supporting electrolytes. The reactor was subjected to

irradiation of 150 W Hg lamps (Oriol) operating under wavelength region in the range of 310-430 nm and 550-575 nm, corresponding to the ultraviolet and visible regions, respectively. The electrochemical reactor was composed of three electrodes system, containing a Pt gauze as counter-electrode, Ag/AgCl, KCl saturated as reference electrode and W/WO₃ as working electrode.

Photoelectrocatalytic measurements

All the measurements related to photocurrents as well as the application of controlled potential were undertaken in a potentiostat/galvanostat Autolab PGSTAT 30 (Eco Chemie) coupled to a system for obtaining data GPES.

The experiments were performed in a photoelectrochemical reactor of approximately 250 mL. The glass reactor was constituted by two concentric compartments (v = 250 mL) with entry to the working electrode, auxiliary electrode, reference electrode, and quartz bubbler tube of 2.5 cm diameter and 15 cm in depth. The reactor has a cooling system between the two compartments, through which a thermostatic bath at 19 °C was used. For the photoexcitation of the material, a mercury vapor lamp Philips 125 W of power was employed.

Following the treatment, solution aliquots were removed and a series of thorough analyses were made including yeast counting, total organic carbon, evaluation of chlorate formation in the system and the investigation of active chlorine formation using spectrophotometric measurements.

Results and Discussion

Morphology and photoactivity of W/WO₃ electrode

The field emission gun-scanning electron microscope (FEG-SEM) images (Figure 1) illustrate a homogenous film formation (Figures 1A, 1B and 1C) with nanopores having average outer diameter around 100 nm and lengths of the order of tens of microns. The X-ray diffraction (XRD) spectra in Figure 1E depicts the diffraction peak. It is worth pointing out the change observed in the W plate after anodizing which is associated with the formation of WO₃ in the monoclinic form. The photoactive form of this oxide was confirmed by the presence of peaks at 2θ = 23.06; 23.71; 24.36; 33.16; 33.65 and 34.00° corresponding to WO₃ in the monoclinic phase.⁴¹ The peaks at 2θ = 40 and 58° are attributed to the metallic W used as substrate. The energy dispersive spectroscopy X-ray (EDX) analysis confirms the presence of the elements that primarily constitute the W/WO₃ electrode, as

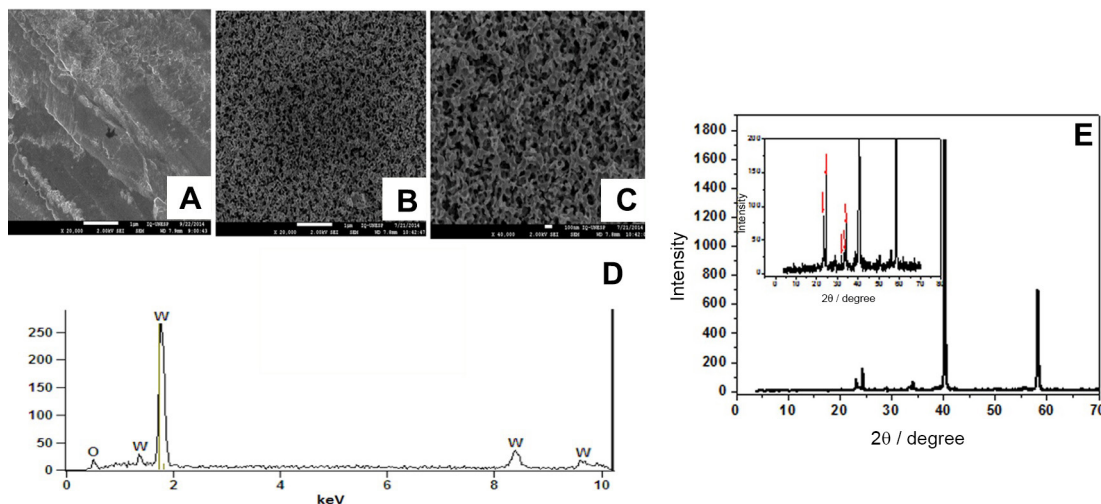


Figure 1. FEM-SEM images of tungsten foil (A) and W/WO₃ prepared by electrochemical anodization of W in NaF 0.15 mol L⁻¹ after 2 h at 60 V amplified 20,000 times (B) and 40,000 times (C). EDX spectra for W/WO₃ nanoporous electrode (D) and X-ray diffraction pattern obtained for the electrode after electrochemical anodization in NaF 0.15 mol L⁻¹ (E).

illustrated in Figure 1D, showing a spectrum that displays peaks with relative intensity, typical of the presence of oxygen (0.6 keV) and W (1.5; 1.7; 8.4 and 9.7 keV). The results indicate that thin films of WO₃ can be easily obtained by electrochemical anodization of W foil in fluoride medium as demonstrated in equations 1-3 which is in accordance with the literature.^{42,43}

Anode:

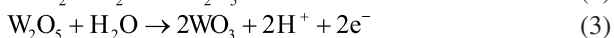
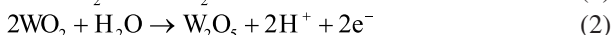
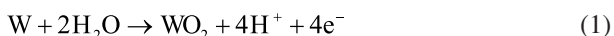


Figure 2 shows the diffuse reflectance spectra of W/WO₃ electrode. The results demonstrate that the material presented high values of optical absorption at wavelengths ≤ 380 nm and well defined bands around 580 nm. This behavior indicates that the material could present a relatively greater advantage once it has the ability to make an excellent use of the irradiated light from a commercial source such as a lamp of 125 W of Hg.⁴⁴

The band gap energy was calculated using Kubelka-Munk function,⁴⁵ as shown in the insert of Figure 2. The W/WO₃ electrode revealed a band gap value of 2.5 eV, close to the commonly reported band gap value for W/WO₃ which is in the range of 2.5-2.8 eV.⁴¹ This behavior contributes to the material absorption towards the visible region.

The photoactivity of the W/WO₃ electrode in sodium sulfate and sodium chloride was evaluated comparing the photocurrent-potential curves under dark conditions (Figure 3, curve a) and under UV-Vis irradiation both in 0.1 mol L⁻¹, pH 7.0. By illuminating the semiconductor with light energy greater than that of the band gap, electron-hole

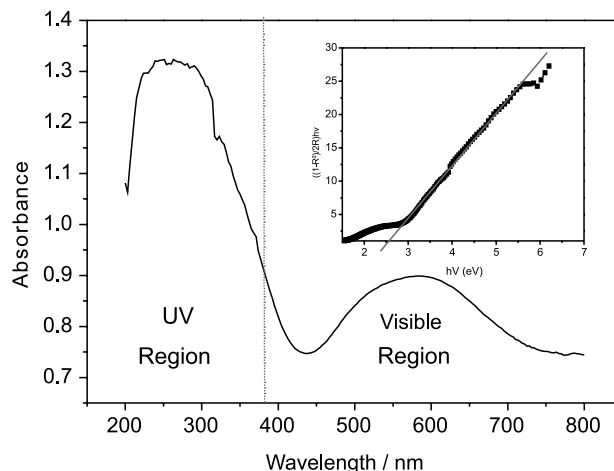


Figure 2. Diffuse reflectance spectra of W/WO₃ electrode with an insert of the band gap of the electrode calculated by Kubelka function and Tauc's graphic.

pairs are found to be generated on the electrode surface. This phenomenon is observed under both visible light and UV-Vis irradiation by applying a bias potential higher than that of the flat band potential of W/WO₃, which in this case is set around +0.10 V vs. Ag/AgCl, calculated using the extrapolation of i_{ph} vs. pH.³² The i_{ph} vs. E curves in NaCl presented larger photocurrent values throughout the results obtained compared to Na₂SO₄ (Figure 3). This behavior is seen to be in line with other studies reported in the literature³¹ and indicates that the photocurrent intensity observed in the sulfate solutions corresponds simply to the contribution of electrons moving towards the counter electrode after their promotion to the conduction band and to the hole generated leading to water oxidation which gives rise to the HO• radicals.^{31,39} Interestingly, chloride ions are known to undergo oxidation during photoelectrocatalysis

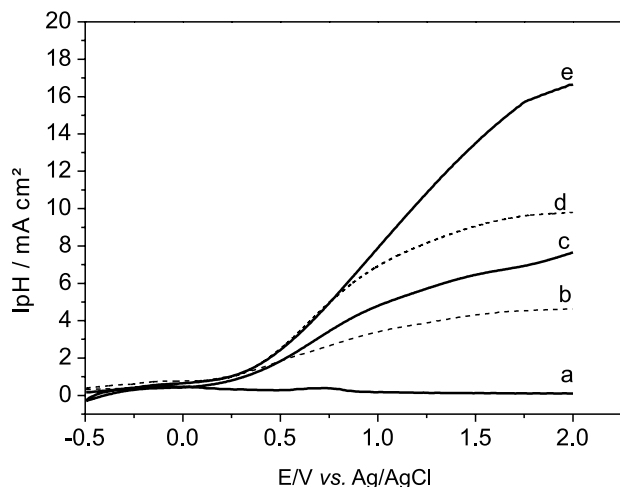
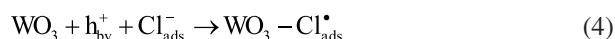


Figure 3. Photocurrent vs. potential curves obtained for W/WO₃ electrode in the dark (a) and under UV-Vis irradiation in Na₂SO₄ (b) and NaCl 0.1 mol L⁻¹ (c), visible light in Na₂SO₄ (d) and NaCl 0.1 mol L⁻¹ (e). pH = 7.0.

in W/WO₃ and Ti/TiO₂ under UV irradiation and positive potential as denoted in equation 4:



Nonetheless, the photocurrent is always seen to bear higher values for UV-Vis irradiation compared to visible light. This can largely be attributed to the fact that the W/WO₃ electrode presents a higher utilization of the radiation emitted by the lamp in the UV and visible regions using the commercial light, as has already been confirmed in the literature.⁴⁴ Thus, it is of no doubt that the use of W/WO₃ anode that promotes a better use of light would bring forth a meaningful contribution once the material is known to be activated by both UV light and visible light emitted by commercial lamp.

Guided by the aim of evaluating the performance of the W/WO₃ electrodes in photoelectrocatalytic disinfection, the NaCl electrolyte performance was compared with that of other electrolytes.

Photoelectrocatalytic measurements

Supporting electrolyte effect

For all the supporting electrolytes considered, 99.99% of *C. parapsilosis* inactivation was observed after 1 min of photoelectrocatalysis under UV-Vis irradiation with E = +1.5 V, as shown in Figure 4A. Additionally, a suspension of *C. parapsilosis* was prepared and maintained without any treatment for two hours (control). The TOC removal reached the range of 85-95% in the presence of Na₂SO₄, NaNO₃ and NaCl as supporting electrolytes (Figure 4B). In all cases, one can observe a slope of the

curve obtained for % TOC removal vs. photoelectrocatalysis time.

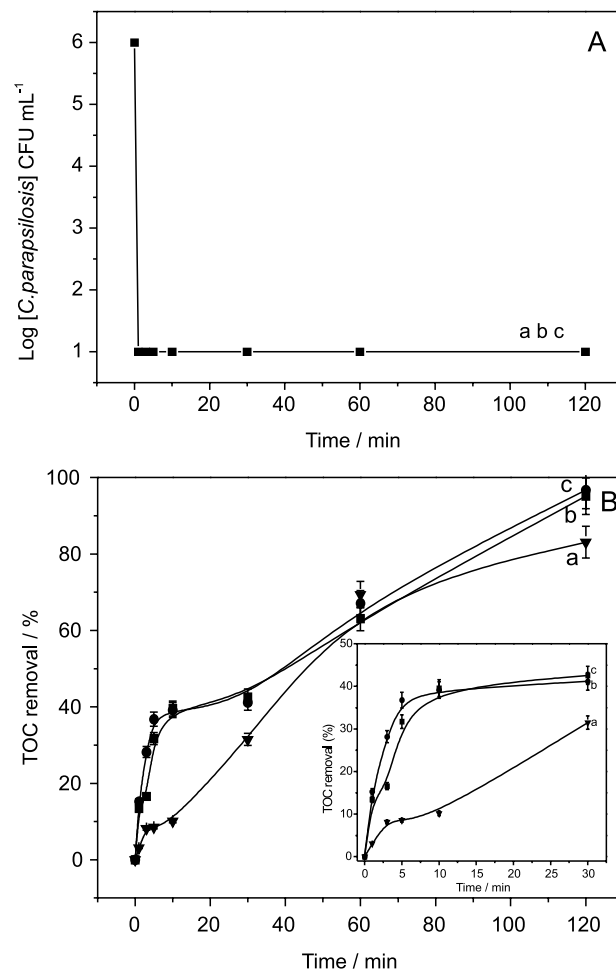


Figure 4. Supporting electrolyte effect in the photoelectrocatalytic treatment of *C. parapsilosis* 1.0 × 10⁶ CFU mL⁻¹ (A) and TOC removal (B) in NaCl (a); Na₂SO₄ (b); and NaNO₃ 0.1 mol L⁻¹ (c). E = 1.5 V vs. Ag/AgCl, irradiation and UV-Vis, 125 W, pH 7.

As reported in the literature,^{35,38,39} the inactivation mechanism of the microorganism is associated with the attack of HO• radicals on the cell wall, where the microorganism-catalyst contact takes place. The fast inactivation observed in all the electrolytes is a clear indication of a rapid formation of hydroxyl radicals in the photoelectrocatalytic system. In addition, the removal of organic material during the treatment evidenced by the TOC removal points to the fact that the attack observed on the cell wall layers leads to the leakage of molecules including glucan and chitin, constituents of the fungal cell wall, which are to be subjected to oxidation. It is worth noting that the damage caused at this stage is seen to be fast and likely to be irreversible, thus leading to the cell death. According to Matsunaga *et al.*,²⁹ the coenzyme A (CoA, CoASH, or HSCoA, is a coenzyme present in the cells, notable for

its role in the synthesis and oxidation of fatty acids, and the oxidation of pyruvate in the citric acid cycle) present in the cells is oxidized by the radicals formed, promoting the inhibition of respiratory activity which consequently paves the way towards the cell death. The degradation of the internal components of the solution during cell lysis may occur subsequently up to almost complete mineralization.

With the aim of understanding the disinfection mechanism in the chloride medium employed as supporting electrolyte, once this is the electrolyte present in higher concentration in the hemodialysis process, it becomes, in essence, crucially important to carry out photoelectrocatalytic disinfection of *C. parapsilosis* in this medium. In order to determine the optimal concentration of NaCl for disinfection of 1.6×10^6 CFU mL⁻¹ *C. parapsilosis*, photoelectrocatalysis was carried out in 0.01, 0.05, 0.1 and 0.2 mol L⁻¹ of NaCl at pH 7.0 using UV-Vis irradiation and an applied potential of +1.5 V. A complete inactivation of *C. parapsilosis* was observed in all the photoelectrolytic measurements undertaken after 1 min of treatment. The TOC results obtained after 60 min of photoelectrolysis are presented in Table 2.

The results obtained after 60 min of treatment indicated that the TOC data show better disinfection rate for concentrations of 0.1 mol L⁻¹ and worst disinfection at 0.01 mol L⁻¹ of NaCl. On the other hand, the best value of TOC removal (around 84%) was observed following 120 min of treatment. The electrolyte is, in essence, important in photoelectrocatalysis owing largely to the influence it exerts when it comes to band bending and charge separation. An increase in the electrolyte concentration tends to improve the junction semiconductor/electrolyte interface, which determines the electron/hole separation kinetics. The junction in a redox electrolyte causes a change in the electrochemical potential (Fermi level) due to discrepant potentials at the interface.⁴⁶ The equilibration of this interface creates a band bending within the semiconductor phase, characterized by the accumulation of electrons or holes on the surface. A maximum influence is clearly observed when 0.05-0.10 mol L⁻¹ of NaCl is

used as electrolyte. Moreover, taking into account that hemodialysis water usually contains 0.10 mol L⁻¹ of NaCl, further studies were carried out choosing this value as the optimum electrolyte concentration.

The microbial death is found to occur rapidly in the first minute of photoelectrocatalytic treatment. The analysis of the behavior of *C. parapsilosis* ($C_0 = 1.0 \times 10^6$ CFU mL⁻¹, $E = +1.5$ V and 0.1 mol L⁻¹ NaCl) during 1 min of treatment is shown in the insert of Figure 4B. Interestingly, the microbial death was found to occur after 30 s of treatment. This result demonstrates the fast inactivation for *C. parapsilosis* by the proposed method.

Effect of pH

The influence of pH (5.0, 7.0 and 8.0) on the disinfection of *C. parapsilosis* ($C_0 = 1.0 \times 10^6$ CFU mL⁻¹, $E = +1.5$ V and 0.1 mol L⁻¹ NaCl) is presented in Table 2. Disinfection was observed in all experimental conditions. Nevertheless, the TOC removal is found to be almost 3 times higher at pH 7 when compared to that observed under pH 8.0, as shown in Figure 5A. In agreement with the literature, the isoelectric point (pzc) of the W/WO₃ electrode was found to be at pH 2.5.⁴⁵ These results indicate that one cannot attribute the behavior observed to the chloride adsorption onto the WO₃ surface, since at pH of 5, 7 and 8 the negative ions are repelled from the WO₃ surface which is found to be negatively charged in these conditions. Oddly enough though, *C. parapsilosis* and water seemed to be adsorbed preponderantly at pH 7.0, increasing the hydroxyl radical generation during the photoelectrocatalytic oxidation process. In all further analyses, pH 7.0 was selected as the optimum pH for the investigation of fungal degradation using chlorine medium, where mineralization and *Candida* sp. disinfection were favorable.

With the purpose of checking whether active chlorine could be formed in these conditions via chloride radical formation (equation 5), further experiments of photoelectrocatalysis were conducted for 1.0×10^6 CFU mL⁻¹ of *C. parapsilosis* in 0.1 mol L⁻¹ NaCl solution at pH 7.0 under UV-Vis

Table 2. TOC removal after 60 minutes of reaction as a function of pH, supporting electrolyte and the applied potential

Influence of pH ^a		Influence of electrolyte ^b		Influence of [electrolyte] ^c		Influence of potential ^d	
pH	TOC removal after 60 min / %	Electrolyte / (0.1 mol L ⁻¹)	TOC removal after 60 min / %	[NaCl] / (mol L ⁻¹)	TOC removal after 60 min / %	Potential / V	TOC removal after 60 min / %
5	54.3	NaCl	63.9	0.01	43.4	+0.7	57.7
7	63.9	Na ₂ SO ₄	63.1	0.5	74.5	+1.0	61.3
8	20.2	NaNO ₃	67.1	0.1	69.9	+1.5	63.9
				0.2	69.6	+2.0	67.6

^a0.1 mol L⁻¹ NaCl, $E = +1.5$ V (vs. Ag/AgCl); ^bpH = 7, $E = +1.5$ V (vs. Ag/AgCl); ^cpH = 7, NaCl, $E = +1.5$ V (vs. Ag/AgCl); ^d0.1 mol L⁻¹ NaCl, pH = 7.

illumination at $E = +1.5$ V, monitored simultaneously with active chlorine generation. Aliquots were removed during 120 min of photoelectrocatalysis and analyzed using the standard colorimetric method based on the *N,N*-diethyl-*p*-phenylenediamine (DPD) indicator for free chlorine.^{20,32} The results obtained showed that an average of 9.00 mg L^{-1} of active chlorine is generated following 20 min of treatment at pH 5.0. These values are seen to be dramatically reduced to 1.56 mg L^{-1} at pH 7 and 8 (Figure 5B). These experiments confirm that active chlorine can be produced at high concentrations on W/WO₃ photoelectrodes in acidic condition though being practically negligible at pH 7 and 8, respectively.

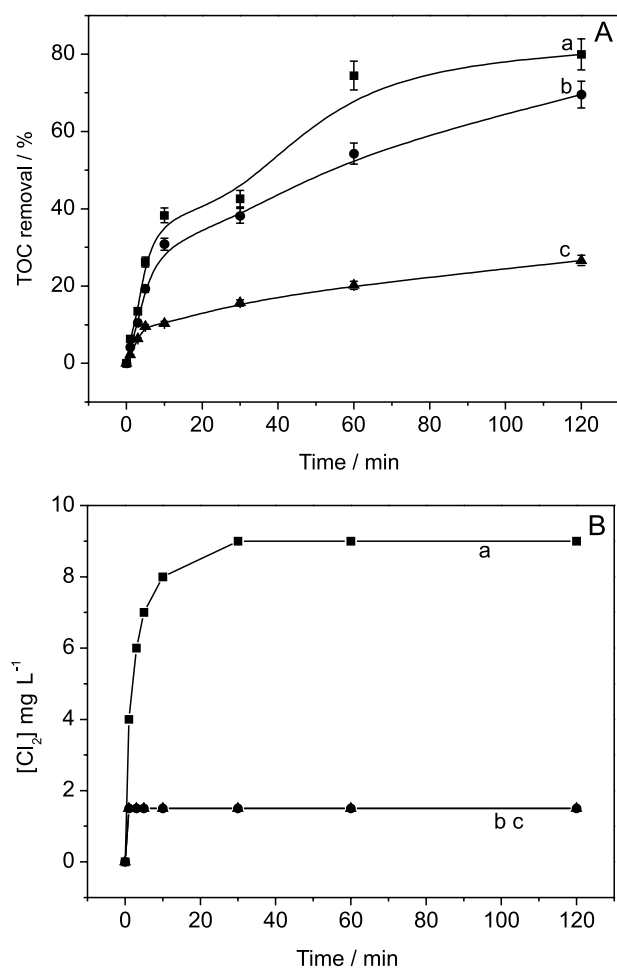


Figure 5. Effect of pH on the TOC reduction during photoelectrocatalytic disinfection of *C. parapsilosis* on W/WO₃ ($E = 1.5$ V vs. Ag/AgCl), NaCl 0.10 mol L^{-1} and UV-Vis irradiation (A) and concomitant active chlorine generation (B). The curves (a), (b) and (c) represent the pH values equivalent to 5, 7 and 8, respectively.

The results obtained indicate that at pH 7, the efficient disinfection observed may be attributed to the improvement of water/*C. parapsilosis* adsorption on the electrode surface even under conditions of high concentrations of

chloride. At higher adsorption conditions, the electron/holes pairs generated at a steady rate lead to the formation of HO• radicals which tend to attack the fungal cell wall, improving the photoelectrocatalytic process because of the minimization of charge recombination. Analysis made by ion chromatography allowed us to observe the non-formation of chlorate and perchlorate ions in the system. Initial measurements of mass spectrometry reveal that there was no formation of organochlorine species. However, this study is still in progress and requires further research.

Effect of applied potential

At potentials above that of the semiconductor flat band which was calculated and being equal to 0.20 V coupled with the application of a potential gradient on the film photoanode, one can observe the death of *C. parapsilosis* after 1 minute treatment for the applied potential ranging from 0.7 to 2.0 V (Table 2). This behavior can be linked to the separation of photogenerated (e^-/h^+) charges that takes place upon the application of UV-Vis irradiation and positive potential. The applied potential acts only to minimize the recombination process, and besides that, any of the applied positive potentials applied towards the disinfection of *C. parapsilosis* is found to be sufficient for the activation of the semiconductor electrode.

Accordingly, the photoelectrocatalytic disinfection was conducted in $1.0 \times 10^6 \text{ CFU mL}^{-1}$ using the best conditions defined previously to verify the importance of selecting the best potential for this process. Potentials ranged between 0.7 to 2.0 V while microbial count and TOC decay were monitored during 120 min of experiment. The results have been summarized in Table 2 showing values obtained after 60 min of treatment. TOC removal is found to increase as a function of the applied potential up to 1.5 V, where maxima values of 80% are reached. Further studies were carried out using 2.0 V as bias potential in photoelectrocatalytic disinfection.

Photoelectrocatalysis vs. photocatalysis and photolysis

In order to test the potentiality of photoelectrocatalysis compared to photocatalysis (UV + semiconductor) and photolysis (UV) *vis-à-vis* the inactivation and degradation of $1.0 \times 10^6 \text{ CFU mL}^{-1}$ of *C. parapsilosis*, experiments were undertaken in NaCl 0.1 mol L^{-1} at pH 7.0 and applied potential of $+1.5$ V. Figure 6 indicates that the microbial counts showed the death of 99.99% of *C. parapsilosis* following one minute of photoelectrocatalytic treatment, 30 min of photocatalysis and 60 min of photolysis. In the three cases considered, we did not observe any formation

of active chlorine, chlorate or perchlorate as subproduct. Furthermore, the mineralization of organic material released from the cell degradation was found to be 83, 30 and 20% for photoelectrocatalysis, photocatalysis and photolysis, respectively (Figure 7).

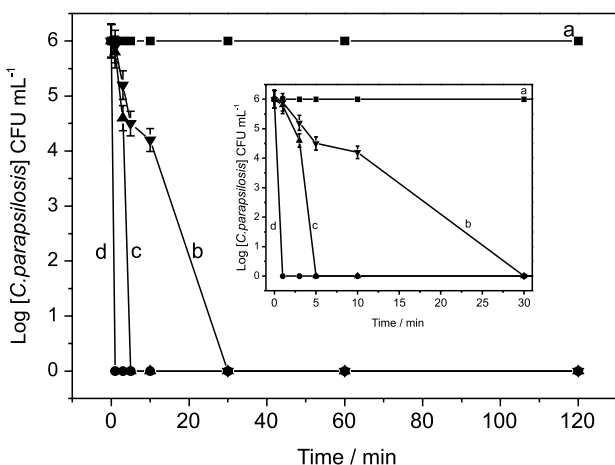


Figure 6. Microbial count for (a) control; (b) photolytic treatment; (c) photocatalytic treatment and (d) photoelectrocatalytic treatment of 1.0×10^6 CFU mL^{-1} *C. parapsilosis* in 0.1 mol L^{-1} NaCl, UV-Vis irradiation, $E = 1.5 \text{ V}$.

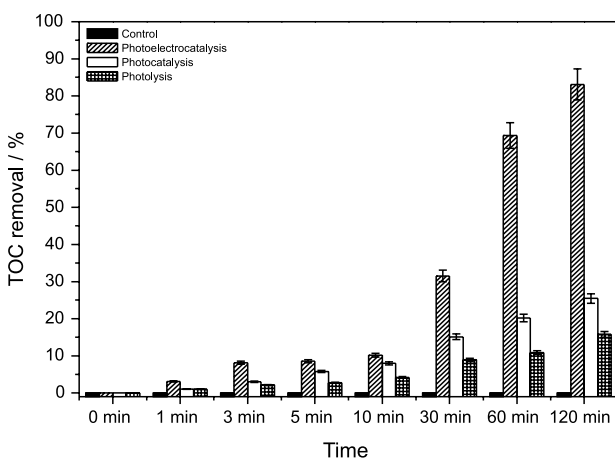


Figure 7. TOC removal for control, photolysis, photocatalysis and photoelectrocatalysis (1.5 eV) of 1.0×10^6 CFU mL^{-1} of *C. parapsilosis* conducted under UV-Vis radiation on W/WO_3 electrode in NaCl 0.10 mol L^{-1} , 125 W , pH 7, and 120 min of treatment.

The $\text{HO}\cdot$ radical is known to be highly toxic to microorganisms and very reactive towards organic substances damaging the nucleic acids and cell wall.⁴⁷ Thus, the presence of only UV light (photolysis), which has a relatively low energy cell damage associated with oxidative stress can be attributed to oxygen radicals inside the cell.⁴⁸ There are different types of DNA damage reported in the literature, among them including the double strand break photo-modification of nitrogenous bases. Nonetheless, these types of damage can be repaired by the cell after a

certain period, which is why a minor disinfection kinetics is observed. When the cell stress exceeds certain threshold, the cell is often seen to die or perhaps becoming incapable of future divisions. The extent of this kind of effect depends on the type of microorganism as well as its history (phase of growth, nutritional status, growth conditions, etc.). The results clearly point out the ineffectiveness of the sole use of photolysis when it comes to the disinfection of *C. parapsilosis*. Furthermore, the degree of performance displayed by photocatalysis is lower compared to photoelectrocatalysis, probably due to the latter's low efficiency in hydroxyl radical generation.

Photoelectrocatalytic treatment of *Candida parapsilosis* under visible irradiation

Guided by the aim of exploring the versatility of W/WO_3 electrodes that present photoactivity in both ultraviolet and visible region besides the advantage of harnessing the material for activation by sunlight which has a higher percentage of visible light, further investigation was carried out following the inactivation and degradation of 1.0×10^6 CFU mL^{-1} of *C. parapsilosis* in 0.1 mol L^{-1} NaCl, pH 7, $E = 1.5 \text{ V}$ under irradiation of UV-Vis and visible light. The microbial counts (Figure 8A) comparing both systems showed that after one minute of treatment, 99.99% of cell death was reached using both visible and ultraviolet radiation. As noted previously and reported in the literature, there was no formation of active chlorine, chlorate or perchlorate during the reaction (results not shown).

Moreover, it can be seen in Figure 8B that 78 and 83% of mineralization were obtained when the treatment was carried out irradiated by visible or UV-Vis light. It can be assumed that photoirradiation of WO_3 films presents high versatility since it has smaller band gap energy ($E_g = 2.5\text{-}2.8 \text{ eV}$), offering better exploitation of the radiation in the visible region. Taking into account the relatively short life span of the hole generated on the electrode surface, it is plausible to say that the active oxygen species ($\text{HO}\cdot$) that likely oxidize the microorganism cell wall are preponderantly generated in this system. Besides that, the material could thus be an alternative proposal for disinfection treatment using visible light as energy source.

Conclusions

Our findings show that photoelectrocatalysis conducted in chloride medium on W/WO_3 electrodes prepared by electrochemical anodization can be used with great success in the deactivation of *Candida parapsilosis*. This study has

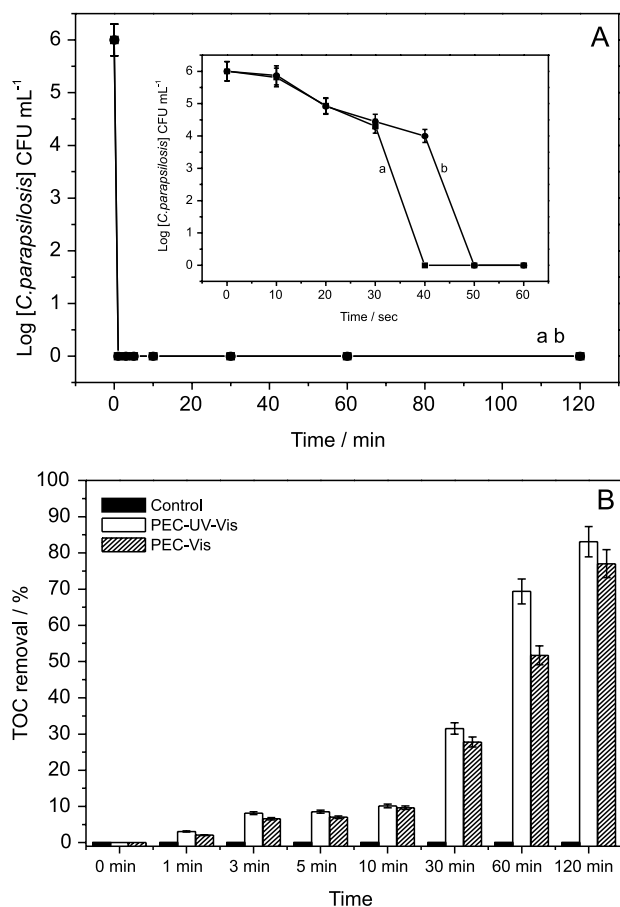


Figure 8. (A) Microbial count for photoelectrocatalytic disinfection of 1.0×10^6 CFU mL⁻¹ *C. parapsilosis* in NaCl 0.1 mol L⁻¹, pH 7.0, UV-Vis irradiation, $E = 1.5$ V for 120 min of treatment and for the initial 60 seconds in the insert; (B) representation of TOC removal for control and photoelectrocatalysis performed with UV-Vis radiation and visible irradiation of W/WO₃ electrode in NaCl 0.1 mol L⁻¹, during 120 min of treatment, $E = 1.5$ V and pH 7.

for the first time unfolded the idea that photoelectrocatalysis conducted at a neutral pH of the initial solution is essentially crucial towards promoting the fungicide effect based on the hydroxyl radical action preponderantly generated in relation to the active chlorine formation as a result of the chloride oxidation. Under optimized experimental conditions of 0.1 mol L⁻¹ NaCl, pH 7, $E = 1.5$ V and UV-Vis irradiation, it is possible to promote total inactivation and around 70-80% of mineralization of organic matter released from cell damage in solution containing *C. parapsilosis* at concentration ranging from 1.0×10^5 to 1.0×10^7 CFU mL⁻¹. Nevertheless, the results obtained through the microbial counts showed that after one minute of treatment, 99.99% inactivation of 1.6×10^6 CFU mL⁻¹ of *C. parapsilosis* was obtained using both visible and ultraviolet radiation. Accordingly, there was no formation of active chlorine, chlorate or perchlorate during the reaction. Although chlorine has been used extensively as

a disinfectant for water purification systems, our method warrants attention and further studies need to be done aiming at applying it in hemodialysis water containing greater amount of chloride in its dialysate fluid given the presence of other components.

Notwithstanding these uncertainties, we believe that the use of W/WO₃ thin-film photoelectrodes prepared by electrochemical methods has proven to be a powerful efficient alternative compared to the usual approaches applied in the disinfection and mineralization of *Candida* spp. of the *Fungi* kingdom in chloride medium. This finding represents undoubtedly a novel meaningful contribution because most of the hemodialysis fluids are found to be easily contaminated by fungus while those available to date, which are used for disinfection, are in most cases based on active chlorine and derivatives.

Acknowledgments

The authors would like to express their deepest gratitude and indebtedness to the Brazilian Research Assistance Agencies FAPESP and CAPES for the financial support granted during the course of this research.

References

- Ministério da Saúde, Portaria No. 2914, de 12 de dezembro de 2011, *Dispõe sobre os Procedimentos de Controle e de Vigilância da Qualidade da Água para Consumo Humano e seu Padrão de Potabilidade*, Brasília, 2011. Available at http://bvsm.s.saude.gov.br/bvsm/saudelegis/gm/2011/prt2914_12_12_2011.html, accessed in March 2017.
- Pires, R. H.; dos Santos, J. M.; Zaia, J. E.; Martins, C. H. G.; Giannini, M. J. M. S.; *Mem. Inst. Oswaldo Cruz* **2011**, *6*, 646.
- Pelczar, M. J.; Chan, E. C. S.; Kriegel, N. R.; *Microbiology*, 5th ed.; McGraw-Hill: New York, 2011.
- Deacon, J. W.; *Fungal Biology*, 4th ed.; Blackwell Publishing: Oxford, 2006.
- Trofa, D.; Gácsér, A.; Nosanchuk, D. J.; *Clin. Microbiol. Rev.* **2008**, *4*, 606.
- Cortia, M.; Solaria, R.; Carolisa, L.; De Cangelosia, D.; Arechavalab, A.; Negronib, R.; *Rev. Iberoam. Micol.* **2013**, *2*, 122.
- Pires, R. H.; Silva, J.; Martins, C. H. G.; Almeida, A. M. F.; Soares, C. P.; Giannini, M. J. M. S.; *Antimicrob. Agents Chemother.* **2013**, *5*, 2417.
- Medrano, D. J. A.; Brilhante, R. S. N.; Cordeiro, R. D. A.; Rocha, M. F. G.; Rabenhorst, S. H. B.; Sidrim, J. J. C.; *Rev. Inst. Med. Trop. Sao Paulo* **2006**, *1*, 17.
- Nosek, J.; Holesova, Z.; Kosa, P.; Gacsér, A.; Tomaska, L.; *Curr. Genet.* **2009**, *5*, 497.

10. Baradkar, V.; Mathur, M.; Rathi, M.; Kumar, S.; *Bombay Hosp. J.* **2008**, *1*, 94.
11. Barbedo, L.; Sgarbi, D. B. G.; *J. Bras. Doenças Sex. Transm.* **2010**, *1*, 22.
12. Valle, G. C.; Rende, J. C.; Okura, M. H.; *NewsLab* **2010**, *101*, 202.
13. Pyrgos, V.; Ratanavanich, K.; Donegan, N.; Veis, J.; Walsh, T. J.; Shoham, S.; *Med. Mycol.* **2009**, *5*, 463.
14. Bessegato, G. G.; Guaraldo, T. T.; Zaroni, M. V. B. In *Modern Electrochemical Methods in Nano, Surface and Corrosion Science*, 1st ed.; Aliofkhaezrai, M., ed.; Intech: Rijeka, 2014, ch. 10, p. 271.
15. Finklea, H. O.; *Semiconductor Electrodes*; Elsevier: New York, 1988.
16. Christensen, P. A.; Curtis, T. P.; Egerton, T. A.; Kosa, S. A. M.; Tinlin, J. R.; *Appl. Catal., B* **2003**, *4*, 371.
17. Egerton, T.; Christensen, P.; *Int. J. Environ. Pollut.* **2006**, *27*, 2.
18. Brugnera, M. F.; Miyata, M.; Zocolo, G. J.; Leite, C. Q. F.; Zaroni, M. V. B.; *Electrochim. Acta* **2012**, *85*, 33.
19. Brugnera, M. F.; Miyata, M.; Leite, F. C. Q.; Zaroni, M. V. B.; *J. Photochem. Photobiol., A* **2014**, *278*, 1.
20. Butterfield, I. M.; Christensen, P. A.; Curtis, T. P.; Gunlazuardi, J.; *Water Res.* **1997**, *3*, 675.
21. Harper, J. C.; Christensen, P. A.; Egerton, T. A.; Curtis, T. P.; Gunlazuardi, J.; *J. Appl. Electrochem.* **2001**, *6*, 623.
22. Egerton, T. A.; Kosa, S. A. M.; Christensen, P. A.; *Phys. Chem. Chem. Phys.* **2006**, *3*, 398.
23. Baram, N.; Starosvetsky, D.; Starosvetsky, J.; Epshtein, M.; Armon, R.; Ein-Eli, Y.; *Electrochim. Acta* **2009**, *12*, 3381.
24. Fraga, L. E.; Anderson, M. A.; Beatriz, M. L. P. M. A.; Paschoal, F. M. M.; Romão, L. P.; Zaroni, M. V. B.; *Electrochim. Acta* **2009**, *7*, 2069.
25. Philippidis, N.; Nikolakaki, E.; Sotiropoulos, S.; Poullos, I.; *J. Chem. Technol. Biotechnol.* **2010**, *8*, 1054.
26. Rahmawati, F.; Kusumaningsih, T.; Hapsari, A. M.; Hastuti, A.; *Chem. Pap.* **2010**, *5*, 557.
27. Pires, R. H.; Brugnera, M. F.; Zaroni, M. V. B.; Giannini, M. J. S. M.; *Appl. Catal., A* **2016**, *511*, 149.
28. Li, G.; Liu, X.; Zhang, H.; Wong, P. K.; An, T.; Zhao, H.; *Appl. Catal., B* **2013**, *140*, 225.
29. Matsunaga, T.; Tomoda, R.; Nakajima, T.; Wake, H.; *FEMS Microbiol. Lett.* **1985**, *1*, 211.
30. Cho, M.; Chung, H.; Choi, W.; Yoon, J.; *Water Res.* **2004**, *4*, 1069.
31. Zaroni, M. V. B.; Sene, J. J.; Anderson, M. A.; *J. Photochem. Photobiol., A* **2003**, *1*, 55.
32. Zaroni, M. V. B.; Sene, J. J.; Selcuk, H.; Anderson, M. A.; *Environ. Sci. Technol.* **2004**, *38*, 11.
33. Jiang, D.; Zhao H.; Zhang, S.; Jonh R.; *J. Phys. Chem.* **2003**, *46*, 12774.
34. Semenikhin, O. A.; Kazarinov, V. E.; Jiang, L.; Hashimoto, K.; Fujishima A.; *Langmuir* **1999**, *11*, 3731.
35. Somasundaram, S.; Chenthamarakshan, C. R.; De Tacconi, N. R.; Basit, N. A.; Rajeshwar, K.; *Electrochem. Commun.* **2006**, *4*, 539.
36. Waldner, G.; Pourmodjib, M.; Bauer, R.; Neumann-Spallart, M.; *Chemosphere* **2003**, *8*, 989.
37. Hepel, M. H. S.; *Electrochim. Acta* **2005**, *25-26*, 5278.
38. Georgieva, J.; Armyanov, S.; Valova, E.; Tsacheva, T.; Poullos, I.; Sotiropoulos, S.; *J. Electroanal. Chem.* **2005**, *1*, 35.
39. Hepel, M.; Luo, J.; *Electrochim. Acta* **2001**, *5*, 729.
40. De Tacconi, N. R.; Chenthamarakshan, C. R.; Yogeewaran, G.; Watcharenwong, A.; de Zoysa, S. R.; Basit, N. A.; Rajeshwar, K.; *J. Phys. Chem., B* **2006**, *50*, 25347.
41. Fraga, L. E.; Zaroni, M. V. B.; *J. Braz. Chem. Soc.* **2011**, *4*, 718.
42. Lai, C. W.; *Sci. World J.* **2014**, 843587.
43. Guaraldo, T. T.; Zaroni, T. B.; de Torresi, S. I. C.; Gonçalves, V. R.; Zocolo, G. J.; Oliveira, D. P.; Zaroni, M. V.; *Chemosphere* **2013**, *5*, 586.
44. Bessegato, G. G.; Cardoso, J. C.; Silva, B. F.; Zaroni, M. V. B.; *J. Photochem. Photobiol., A* **2013**, *276*, 96.
45. Anik, M.; Cansizoglu, T.; *J. Appl. Electrochem.* **2006**, *36*, 603.
46. Bessegato, G. G.; Cardoso, J. C.; Zaroni, M. V. B.; *Catal. Today* **2015**, *240*, 100.
47. Ozyildiz, F.; Golden, M.; Uzel, A.; Karaboz, I.; Akil, O.; Bulut, H.; *Biotechnol. Bioprocess Eng.* **2010**, *4*, 680.
48. Bock, C.; Dittmar, H.; Gemeinhardt, H.; Bauer, E.; Greulich, K. O.; *Mutat. Res., DNA Repair* **1998**, *2*, 111.

Submitted: October 20, 2016

Published online: March 21, 2017